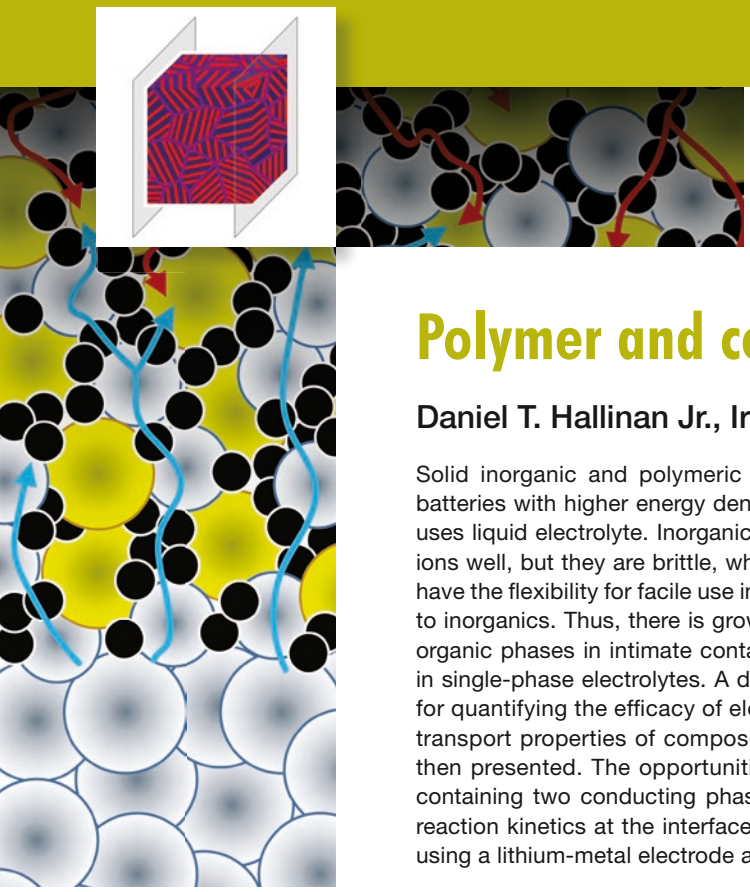

Polymer and composite electrolytes

Daniel T. Hallinan Jr., Irune Villaluenga, and Nitash P. Balsara

Solid inorganic and polymeric electrolytes have the potential to enable rechargeable batteries with higher energy densities, compared to current lithium-ion technology, which uses liquid electrolyte. Inorganic materials such as ceramics and glasses conduct lithium ions well, but they are brittle, which makes incorporation into a battery difficult. Polymers have the flexibility for facile use in a battery, but their transport properties tend to be inferior to inorganics. Thus, there is growing interest in composite electrolytes with inorganic and organic phases in intimate contact. This article begins with a discussion of ion transport in single-phase electrolytes. A dimensionless number (the Newman number) is presented for quantifying the efficacy of electrolytes. An effective medium framework for predicting transport properties of composite electrolytes containing only one conducting phase is then presented. The opportunities and challenges presented by composite electrolytes containing two conducting phases are addressed. Finally, the importance and status of reaction kinetics at the interfaces between solid electrolytes and electrodes are covered, using a lithium-metal electrode as an example.

Introduction

In their prophetic 1980 paper, Mizushima, Jones, Wineman, and Goodenough provided the first evidence of reversible lithium intercalation in a 4 V cathode (Li_xCoO_2).[1] They proposed the "use of a solid electrolyte of large breakdown voltage to enable a greater fraction of the potential energy density to be utilized." Experiments in this work were done using a liquid electrolyte: a mixture of a lithium salt (lithium tetrafluoroborate) and propylene carbonate. Harris and Tobias[2] first proposed the possibility of using alkyl carbonates as solvents for lithium salts in batteries. This class of electrolytes also enables reversible intercalation into and out of graphite, as shown by Fong, VonSacken, and Dahn.[3] The lithium-ion battery used today is built on these three discoveries.

The main motivation that drives the development of solid electrolytes today is the possibility of increasing energy density by replacing the graphite anode with a lithium foil, as Goodenough and co-workers recognized. Two classes of solid electrolytes have emerged: mixtures of salts and organic polymers, and inorganic materials—ceramics and glasses—that contain mobile lithium ions.

The field of polymer electrolytes began with the work of Fenton, Parker, and Wright, who discovered that alkali salts dissolve in poly(ethylene oxide) (PEO).[4] PEO, which is a semicrystalline solid at room temperature, is only conductive at temperatures above the melting temperature (60°C).[5] Above the melting temperature, PEO is a viscoelastic liquid; the linear chains undergo Brownian motion on a time scale that is dictated by chain length.[6] The conventional approach to "solidifying" viscoelastic chains is chemical cross-linking.[7] Inorganic solids that conduct lithium ions have been identified for lithium batteries.[8–12] In such crystalline solids, lithium ions hop from one unit cell to the next, and the motion of the ions depends on the activation barrier along the transport pathway. The motion of ions through inorganic glasses is similar, except for the fact that the atoms surrounding the mobile ions are not arranged on a well-defined lattice. Some inorganic solids exhibit room-temperature conductivity comparable to that of liquid electrolytes.[10]

The properties of different solids can be combined in composite electrolytes. Block copolymers, wherein a PEO chain is covalently bonded to a rigid polymer such as polystyrene (PS), are one example. The PS chains are trapped in the glassy domains and the covalent bond prevents Brownian motion of the PEO chains. The presence of rigid nonconducting domains (all known dry lithium-ion-conducting polymers are rubbery) reduces conductivity, but can lead to a dramatic increase in the modulus of the electrolyte. One approach to stabilize the lithium metal anode is through the use of rigid solid electrolytes.[13] Building robust rechargeable batteries with brittle

Daniel T. Hallinan Jr., Florida A&M University–Florida State University, USA; dhallinan@fsu.edu
Irune Villaluenga, Blue Current, USA; irvillaluenga@gmail.com
Nitash P. Balsara, University of California, Berkeley, USA; nbalsara@berkeley.edu
doi:10.1557/mrs.2018.212

inorganic crystalline and glassy materials is challenging. Additionally, maintaining electrical contact between the electrolyte and the active particles is difficult due to volume changes that accompany the redox reactions. These obstacles may be overcome through the design of polymer-inorganic hybrid electrolytes wherein the role of the polymer is to endow the electrolyte with ductility and adhesive properties that are necessary for battery manufacturing and operation. In this class of composite electrolytes, both phases need to conduct ions.

This article addresses polymer electrolytes and composites. Our discussion of composites begins with a discussion of block copolymer electrolytes, focusing on the effects of nonconducting domains on ion transport through a polymer. We then discuss composites of polymers and ion-conducting inorganic materials wherein ion transport can, in principle, occur in both phases. The ultimate goal of an electrolyte is to enable redox reactions. We thus conclude with a discussion of reaction kinetics at the interface between solid electrolytes and redox-active solids.

Single-phase polymer and inorganic electrolytes

The number of transport coefficients needed to fully characterize ion transport in an n-component mixture is $n(n-1)/2$.[14] In this respect, polymer electrolytes such as mixtures of linear PEO chains and a lithium salt are similar to liquid electrolytes. These binary electrolytes contain three species: the cation, the anion, and the "solvent." They are characterized by three transport coefficients ($n = 3$): ionic conductivity, κ (or κ_c) measured using ac impedance, salt diffusion coefficient, D (or D_c) measured using restricted diffusion, and the cation transference number, t_+^0 (or t_{+c}^0) measured by either the current-interrupt method[15] or the steady-state current method.[16] The cation transference number is defined as the fraction of current carried by the cations under an applied potential in the absence of a concentration gradient. In addition, ion transport depends on the thermodynamic factor, $T_h = (1+ d\ln\gamma_\pm/d\ln m)$, where $\gamma_\pm$ is the mean molal activity coefficient of the salt and m is the molality of the conducting phase. These parameters for mixtures of PEO (molecular weight, M, 5 kg/mol) and lithium bis(trifluoromethanesulfone)-imide (LiTFSI) are given in **Table I** at $m = 1.4$ and 3.6 mol/kg at 90°C. Experiments have shown that κ is independent of polymer molecular weight when M exceeds 5 kg/mol.[17,18] We expect the same to hold for D, t_+^0, and T_h.

The parameters, κ, D, t_+^0, and T_h of PEO/LiTFSI are strong functions of salt concentration;[16] we have chosen to show data obtained at particular salt concentrations for purposes of illustration. The second law of thermodynamics requires κ, D, and T_h to be positive. At $m = 1.4$ mol/kg, t_+^0 of PEO/LiTFSI is positive, the usual case for most electrolytes. However, at $m = 3.6$ mol/kg, t_+^0 is negative. Since $t_+^0 + t_-^0 = 1$ by definition, the anion transference number, t_-^0, for the PEO/LiTFSI electrolyte at $m = 3.6$ kg/mol in Table I is 1.4. The second law of thermodynamics places no bounds on either t_+^0 or t_-^0. Table I also shows data on a less-studied electrolyte wherein LiTFSI is dissolved in a perfluoropolyether (PFPE).

The performance of an electrolyte in a battery depends on its ability to sustain a current under an applied potential. Measurements of this important parameter were first made by Bruce and Vincent[19] and Watanabe et al.[20] Newman and co-workers[14,21,22] have shown that the current under a small applied constant potential is governed by the dimensionless parameter, Ne, defined for univalent salts as:

$$\mathrm{Ne} = \frac{2\kappa TRT_h(1-t_+^0)^2}{F^2 Dc}. \quad (1)$$

Here, R, T, and F are the gas constant, temperature, and Faraday's constant, respectively. The variable c is the salt concentration expressed in molarity. We propose calling the nondimensional parameter defined by Equation 1 the Newman number, in recognition of the central role that J. Newman has played in deriving Equation 1 and for his pioneering efforts to characterize ion transport in electrochemical systems.[14,21,22]

The steady-state current in any homogeneous electrolyte (liquid or solid) under a small applied constant potential (i.e., constant transport coefficients can be assumed) is proportional to $\kappa/(1 + \mathrm{Ne})$. This enables direct determination of Ne if other transport parameters in Equation 1 are not known.[16] Values of Ne and $\kappa/(1 + \mathrm{Ne})$ for PEO/LiTFSI and PFPE/LiTFSI are given in Table I.

It is, perhaps, important to discuss the consequences of transference numbers that are less than 0 (or greater than 1). For an electrolyte subjected to a small constant potential in a symmetric lithium-electrolyte-lithium cell, a negative value for t_+^0 implies that migration drives both the cation and the anion toward the same electrode. For the case of PEO/LiTFSI at $m = 3.6$ mol/kg, migration drives the Li^+ ions toward the positive electrode while diffusion drives the Li^+ ions toward the negative electrode. The net flux of Li^+ ions is always toward the negative electrode where they are consumed by the electrochemical reaction; Ne is always positive, even if t_+ is less than zero or greater than unity (see Equation 1).

The last pure electrolyte listed in Table I is an inorganic lithium-phosphorus-sulfur (LPS) glass ($x\mathrm{Li_2S}.(100 - x)\mathrm{P_2S_5}$ (mol%)) developed by Zhang and Kennedy;[12] data are taken from Reference 23. In this electrolyte, $t_+^0 = 1$. For electrolytes with $t_+^0 = 1$, Ne = 0 (see Equation 1). The material contains only one mobile charge carrier in a matrix ($n = 2$), and the number of transport parameters needed to predict the properties of these electrolytes is 1, usually κ. Polymers with anions that are covalently bonded to the chains and free lithium counterions are also examples of single-ion conductors.[24–26]

The properties of electrolytes are affected by temperature, following the Arrhenius or Vogel–Fulcher–Tammann (VFT) equation.[27] Ion transport in PEO electrolytes depends on the crystallization and glass-transition temperatures, T_c and T_g. The effect of these parameters on κ has been studied extensively—κ increases sharply above T_c and increases with

Table I. Transport properties of selected polymer and composite electrolytes at 90°C.

System	m (mol/kg)	ϕ_c	D (cm²/s)	κ (S/cm)	t_+^0	T_h	Ne	$\kappa/(1 + Ne)$ (S/cm)
PEO/LiTFSI	1.4	1	1.3×10^{-7}	2.0×10^{-3}	+0.3	2.1	8.6	2.1×10^{-4}
PEO/LiTFSI	3.6	1	9.4×10^{-8}	1.3×10^{-3}	–0.4	2.3	15.7	7.8×10^{-5}
PFPE/LiTFSI	0.3	1	NM	1.9×10^{-5}	NM	NM	0.1	1.7×10^{-5}
LPS	ND	1	ND	1.4×10^{-3}	+1.0	ND	0	1.4×10^{-3}
SEO/LiTFSI	1.4	0.54	5.4×10^{-8}	4.9×10^{-4}	–0.5	1.1	21.4	2.2×10^{-5}
SEO/LiTFSI	3.6	0.60	3.2×10^{-8}	5.1×10^{-4}	+0.2	3.2	13.7	3.5×10^{-5}
LPS+ PFPE/LiTFSI	ND	1	NM	1.1×10^{-3}	+0.99	NM	0.01	1.1×10^{-3}

Note: PEO, poly(ethylene oxide); LiTFSI, lithium bis(trifluoromethanesulfone)-imide; PFPE, perfluoropolyether; LPS, lithium-phosphorus-sulfur; SEO, polystyrene-*block*-polyethylene oxide electrolyte; Ne, dimensionless number that we propose to call the Newman number; ϕ_c, volume fraction of the conducting phase; NM, not measured; ND, not defined.

increasing temperature in accordance with the VFT equation.[27] The addition of salt to PEO decreases T_c and increases T_g. In practical applications, batteries containing PEO-based electrolytes are run at elevated temperatures (e.g., 70 or 90°C [above both T_c and T_g]). This is not a concern for electric vehicle applications. In fact, thermal management for such a battery is simpler and cheaper than battery management systems for lithium-ion technology wherein the battery must be cooled to maintain temperatures below 35°C. The main limitation with PEO-based electrolytes is that with the addition of salt, T_g of the electrolytes increases and this decreases conductivity; the T_g of PEO increases from –56 to –27°C when m is increased from 0 to 3.6.[28,29] Batteries with PEO electrolytes cannot be operated at room temperature at high rates, not because they are crystalline, but because of the proximity of T_g to room temperature.

Composite electrolytes with one conducting domain

A composite electrolyte has two distributed phases. We first focus on composite electrolytes in which only one of the phases conducts ions (the other phase is an insulator). Examples include a polymer electrolyte matrix filled with nonconducting ceramic particles, conducting particles bound in a nonconducting elastomer, and block copolymers in which one microphase conducts ions and the other does not. Nanoparticles (whether conducting or not) commonly take the form of spheres, rods, or platelets. A diblock copolymer is obtained by covalently linking two chemically distinct chain molecules. In the bulk, these molecules self-assemble into ordered morphologies comprising spheres, cylinders, or lamellae, depending on the volume fraction of the conducting block. The ability to use molecular structure to tune morphology makes block copolymers ideal for quantifying the effect of composite structure on ion transport. A typical block-copolymer electrolyte is shown in **Figure 1**. Here, we show randomly oriented grains; each grain comprises coherently ordered conducting and nonconducting lamellae.

The most widely studied block copolymer electrolytes for lithium batteries are based on PS and PEO chains (SEO). This block copolymer is mixed with a lithium salt, which more-or-less partitions exclusively into the PEO microphase. The PEO-rich domains thus conduct lithium ions (see previous section) while the glassy and rigid PS microphase provides mechanical strength.[30] Effective-medium theory,[31] developed by Sax and Ottino to describe gas transport in composite membranes, can be used to predict ion transport in block copolymer electrolytes in which the conducting phase is the minority component.[27] This framework predicts transport through a collection of randomly oriented grains. This approach is valid when the transport path is much larger than the grain size and when the resistance to transport between grains is negligible.

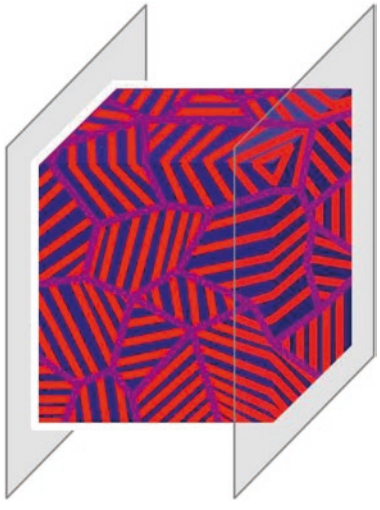

Figure 1. Morphology of a composite block copolymer electrolyte with randomly oriented grains. Each grain comprises alternating conducting and nonconducting lamellae. We are interested in ion transport between two electrodes, shown as thin plates in the figure.

The conductivity of a composite (κ) should increase with the conductivity of the pure conducting phase (κ_c) and the volume fraction of the conducting phase (ϕ_c). (Subscript c refers to the pure conducting phase for all variables.) In the simplest case, these increases are linear,

$$\kappa = \frac{f}{\tau}\phi_c\kappa_c, \quad (2)$$

where f is the morphology factor and τ is the tortuosity. The morphology factor arises because certain grain orientations do not contribute to ion transport in the desired direction. The dependence of block copolymer morphology on composition (ϕ_c) is well established. **Table II** lists morphologies that are obtained as ϕ_c increases. We begin by discussing composites with low ϕ_c (i.e., systems wherein the majority component is insulating). For simplicity, we show grains oriented along the x, y, and z directions of a Cartesian coordinate system oriented along the desired direction of transport. Also given in Table II are values of f and τ^{-1} for each morphology. In the trivial case wherein the conducting phase takes the form of isolated spheres, no orientation allows macroscopic ion transport, and f is 0.

One out of three cylindrical grains contributes to transport, while two out of three lamellar grains contribute to transport. Thus, for cylinders and lamella, f is 1/3 and 2/3. The calculations of Sax and Ottino averages over all possible orientations of lamellar and cylindrical grains.[31] The final results of these calculations are identical to those presented here based on simple arguments. In a narrow composition window between cylinders and lamellae, block copolymers form triply connected networks called the gyroid phase. Here, all grains contribute to transport and f is 1. However, the path of the ions is tortuous in this case. The tortuosity of the network in the block copolymer gyroid phase was recently shown to be a weak function of ϕ_c, and τ^{-1} was found to be approximately 1/2 and 4/5 when the network is the minority and majority phase, respectively.[33]

The matrix in block copolymers with $\phi_c > 0.676$ is conducting, and $f = 1$ in this regime. The tortuosity of a composite comprising a conducting matrix and randomly placed insulating spheres was derived by Maxwell[35]

$$\tau^{-1} = \frac{d-1}{(d-\phi_c)}. \quad (3)$$

Equation 3 applies in the limit of dilute, insulating spheres ($d = 3$) and cylinders ($d = 2$).[36] This gives τ^{-1} for the sphere and cylinder phases at high ϕ_c in Table II.

Ion transport in a composite with one conducting phase is described by the same three transport coefficients and the same thermodynamic factor that are used to describe homogeneous binary electrolytes. The salt diffusion coefficient is given by:

Table II. Morphology and tortuosity factors for transport in ion-conducting block copolymers with specified morphology.[32]

Morphology		f	τ^{-1}	Ref.
Conducting Spheres	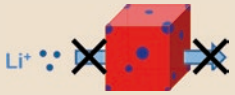	0	1	27
Conducting Cylinders	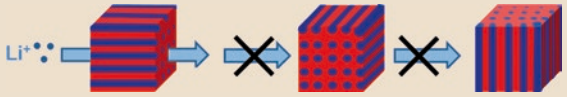	1/3	1	27
Conducting Minor Gyroid	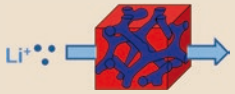	1	1/2	33
Lamellae	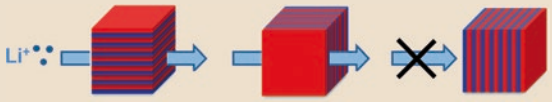	2/3	1	27
Conducting Gyroid Matrix	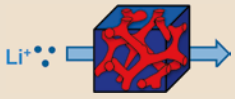	1	4/5	33
Cylinders in Conducting Matrix	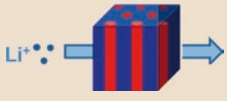	1	$\frac{1}{2-\phi_c}$	34
Spheres in Conducting Matrix	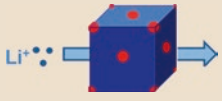	1	$\frac{2}{3-\phi_c}$	34

An X over an arrow indicates that ion transport does not occur in the specified direction.

$$D = \frac{f}{\tau} D_c . \quad (4)$$

The rationale for Equation 4 (absence of ϕ_c in the equation) is straightforward. Imagine an experiment wherein one creates a salt concentration gradient in a single lamellar grain by applying an electric field with suitable electrodes, and studies the relaxation of this gradient. This relaxation will be affected by f and τ, due to the morphology and orientation of the grain, but not ϕ_c. Similar arguments lead to the conclusion that t_+^0 and T_h are affected by neither f, nor τ, nor ϕ_c.

$$t_{+c}^0 = t_+^0 \text{ and } T_{hc} = T_h . \quad (5)$$

The Newman number for a composite can then be expressed in terms of the transport properties of the composite as:

$$\mathrm{Ne} = \frac{2\kappa T R T_h (1 - t_0^+)^2}{F^2 D c \phi_c}, \quad (6)$$

where c is the salt concentration in the conducting phase.

The conductivity (κ) and diffusivity (D) of composite electrolytes depend crucially on $f\tau^{-1}$. The dependence of this parameter for block copolymer electrolytes on ϕ_c is shown in **Figure 2**. The volume fractions at which morphological changes occur are from calculations for a neutral (ion-free) block copolymer that is strongly segregated ($\chi N = 80$, where χ is the Flory–Huggins interaction parameter and N is the chain length).[37,38]

Complete electrochemical characterization of a block copolymer electrolyte has been recently completed.[39] The results

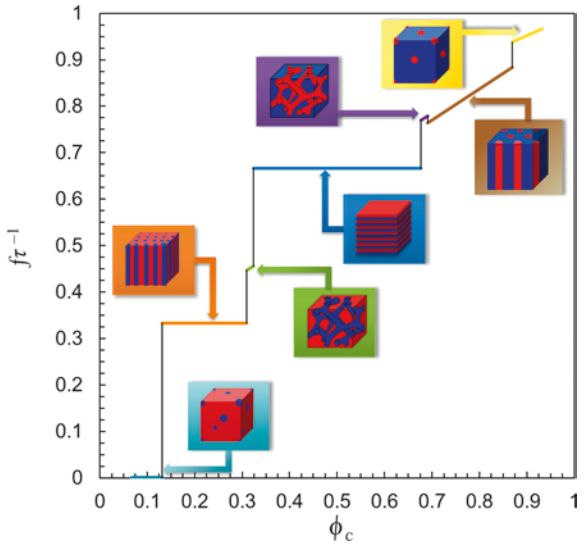

Figure 2. The ratio of the morphology factor, f, and tortuosity, τ, for composite block copolymer electrolytes with one conducting phase as a function of the volume fraction of that phase. Includes conducting spheres, conducting cylinders, conducting minor gyroid, lamellae, conducting gyroid matrix, cylinders in conducting matrix, and spheres in conducting matrix. All transport properties of the composite can be estimated using this plot.

obtained for a lamellar SEO block copolymer electrolyte with ϕ_c in the vicinity of 0.5 is included in Table I. The salt concentration in the PEO lamellae is calculated under the assumption that all of the added salt partitions into the PEO lamellae. The model presented here predicts that $\kappa/\phi_c\kappa_c = D/D_c = f/\tau = 0.67$, and $t_+^0/t_{+c}^0 = T_h/T_{hc} = 1$. The data in Table I are not in agreement with this expectation. For $m = 1.4$, $\kappa/\phi_c\kappa_c = 0.45$, $D/D_c = 0.42$, $t_+^0/t_{+c}^0 = -1.67$, and $T_h/T_{hc} = 0.52$. For $m = 3.6$, $\kappa/\phi_c\kappa_c = 0.66$, $D/D_c = 0.34$, $t_+^0/t_{+c}^0 = -0.50$, and $T_h/T_{hc} = 1.39$. These results suggest that the intrinsic ion transport properties of salt-containing microphases in block copolymer electrolytes differ significantly from those of pure homopolymer electrolytes. One issue is that the transport coefficients (particularly t_+^0) are sensitive functions of m. If the distribution of salt in PEO is affected by the presence of other phases, then one may expect more complex relationships between the transport properties of block copolymer and homopolymer electrolytes. The present discussion is a simple starting point for understanding the factors that govern ion transport in composite electrolytes.

Composites comprising insulating nanoparticles such as silica or titania in PEO/salt mixtures have been studied extensively. Early work suggested that these composites had significantly higher conductivity than the pure electrolyte; at some compositions the reported composite conductivity was three orders of magnitude higher.[40] The framework presented in this article does not support these results. Most of the work that followed the original studies has shown that the conductivity of amorphous PEO/salt mixtures with and without added nanoparticles are similar.[41] Work from our laboratory has shown that adding titania nanoparticles reduces the conductivity of block copolymer electrolytes.[42] One of the problems with nanoparticle/polymer mixtures is aggregation of the particles driven by depletion interactions.[43] The morphology of these composites can thus evolve with time at temperatures above the T_g of the polymer electrolyte.

The morphology of many composites made by conventional blending processes such as ball-milling or slurry casting is more complex than the ideal morphologies shown in Table II. In such cases, it is customary to use empirical relationships such as the Bruggemann equation to evaluate τ (assuming $f = 1$).[44]

$$\tau = \beta \phi_c^{1-\alpha}, \quad (7)$$

where β and α are empirically determined parameters. β is often taken as 1 and α as 1.5.[45]

Composite electrolytes with two conducting domains

It is not difficult to imagine composite electrolytes with the geometries described in Table II wherein both phases are ionic conductors. There are a few inorganic glass-ceramics and crystals with conductivities that are in the vicinity of 10^{-2} S/cm ($70Li_2S.30P_2S_5$ glass-ceramic, $Li_{10}GeP_2S_{12}$, and $Li_{9.54}Si_{1.74}P_{1.44}S_{11.7}Cl_{0.3}$) at room temperature.[10,46,47] The motivation for blending a polymer with inorganic particles is to

address the limitations of pure inorganic materials, which are brittle and difficult to process. Very little is known about such systems at this time. The simplest composite is one wherein both phases are single-ion conductors (Ne = 0). Ion transport in such systems is fully characterized by κ. Since the ion of interest traverses both phases, and particular grain orientations do not forbid transport, a simple starting point is to assume that κ of the composite is given by a volume-fraction-weighted mean of the conductivities of the phases. Assuming that the composite comprises particles dispersed in a matrix,

$$\kappa = \phi_m \kappa_m + (1-\phi_m)\kappa_p, \tag{8}$$

where κ_i is the conductivity of phase i ($i = m$ for matrix and p for particle). Equation 8 would apply to materials containing parallel transport pathways through both phases. For conducting particles dispersed in a conducting matrix, more sophisticated analysis of charge transport was done by Maxwell, leading to the generalized equation:

$$\frac{\kappa}{\kappa_m} = \frac{\left[d(1-\phi_m)+\phi_m\right]\frac{\kappa_p}{\kappa_m} + (d-1)\phi_m}{\phi_m \frac{\kappa_p}{\kappa_m} + (d-\phi_m)}, \tag{9}$$

where spherical (dimension, $d = 3$) or cylindrical ($d = 2$) particles are included. For the cylinder case, it is assumed that the cylinders are long with axes oriented normal to the transport direction, and thus ion transport reduces to a two-dimensional problem. For the case of long and wide platelets ($d = 1$), Equation 9 reduces to the volume-fraction-weighted harmonic mean, which applies to materials containing transport pathways in series. If the fraction of parallel and series pathways is known, such as in block copolymers, Equations 8 and 9 can be combined appropriately.[31]

If the phases that make up the composite electrolyte are different binary electrolytes comprising the same lithium salt, then $n = 4$. If a single-ion conductor is dispersed in a binary polymer electrolyte, then n is also equal to 4. In these cases, six transport coefficients are necessary to describe ion transport in these composites. It is not clear what these transport coefficients are or how they might be measured. Additional parameters related to interfacial transport, particularly due to the mismatch in t_+^0, may need to be introduced.

Strangely, addition of single-ion conducting particles at low volume fractions has not shown significant conductivity enhancements in polymer electrolyte.[48] Similarly, at high particle volume fractions, the use of a conducting polymer binder does not improve conductivity beyond that found when conductive particles are bound by an inert polymer.[49] The major impediment is thought to be large interfacial resistance between conductive particles and conductive polymer.[50] Experiments show that as the particle volume fraction is increased, the lithium-ion-transport pathway transition from purely through the polymer matrix to purely through percolated particles.[51]

The large interfacial resistance between polymer and ceramic conductors is likely to arise due to a transference number mismatch. The ceramic particles are single-ion conductors, whereas both cations and anions are mobile in PEO electrolytes. At low particle volume fractions, the particle cannot contribute to conduction because anions must diffuse with Li^+ in order to maintain electroneutrality. As depicted schematically in **Figure 3**, the necessity for anions, X^-, to diffuse around particles limits transport of Li^+. Even if Li^+ were to diffuse through the particle, it would need to "wait" for the anion. This transference number mismatch is manifested as polarization losses in cells containing a laminated electrolyte comprising a binary electrolyte and a single-ion conductor in series.[52] Such polarization losses have been modeled using the concept of charge-transfer reaction (discussed in more detail in the next section).[53]

These arguments regarding transference number mismatch are supported by results of a recent study that combined a single-ion conducting polymer electrolyte with conducting particles.[23] This composite was based on LPS glass electrolyte and PFPE/LiTFSI polymer electrolyte (the last entry in Table I). The conductivity of the composite was predicted by the volume-fraction-weighted average of the conductivities of the neat components. The values of ionic conductivity predicted are similar to those obtained experimentally. The term κ/(1 + Ne) for this composite is very close to the value of single-ion conductor LPS electrolyte, which corresponds to the highest value in Table I.

Reaction kinetics at solid-electrolyte–electrode interfaces

Just as the ion transport previously described is important in the bulk of electrolytes, reaction kinetics dictate behavior at the electrolyte–electrode interface. When ions reach the boundaries of an electrolyte (whether solid or liquid), they are consumed or generated via reaction with an electrode. In fact, it is the consumption at one electrode and generation at the other electrode that drives a current through a battery. Complete understanding of an electrolyte's performance in a battery therefore requires knowledge of the electrochemical reaction kinetics. To measure reaction kinetics, it is important to achieve conditions in which the reaction is rate limiting. Two kinetic processes occur shortly

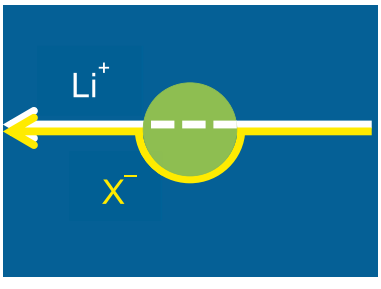

Figure 3. Schematic of a composite electrolyte with single-ion conducting particles and binary polymer electrolyte matrix.

(less than 10 ms) after the imposition of current—ohmic resistance dictated by κ and capacitive charging of the electric double layer. Then, the reaction kinetics tends to be rate limiting until a concentration gradient develops in the electrolyte due to mass transport limitations. The challenge is usually identifying conditions in which the reaction, rather than mass transport, limits kinetics. In single-ion conductors in which concentration gradients do not develop, this is trivial.

In binary liquid electrolytes, this challenge is traditionally met with a rotating disk electrode (RDE), which convectively mixes the electrolyte, minimizing concentration gradients so that reaction kinetics are rate limiting.[54] Convective mixing is not possible in solid electrolytes, but there are other methods for determining the exchange current density, i_0, which represents the electrochemical reaction rate at equilibrium.[54]

Regardless of the experimental technique, current versus voltage data is analyzed with an appropriate reaction model, such as the Butler–Volmer model for an elementary, one-electron reaction between an oxidized and a reduced species, $O + e^- \underset{k_a}{\overset{k_c}{\rightleftharpoons}} R$. Taking a lithium metal electrode as an example, $O = Li^+$ and $R = Li$. The Butler–Volmer model can then be expressed as follows:[14]

$$i = i_0\left[\exp\left(\frac{\alpha_a F\eta}{RT}\right) - \exp\left(\frac{\alpha_c F\eta}{RT}\right)\right], \quad (10)$$

where i is the net current density (mA/cm^2). Under open-circuit conditions in an electrochemical cell ($i = 0$), both oxidation and reduction reactions occur at equal rates. i_0 is proportional to a rate constant used in ordinary chemical reaction kinetics, k_0 (cm/s), according to:

$$i_0 = Fk_0 c_o^{\alpha_c} c_R^{\alpha_a}, \quad (11)$$

where c_O and c_R are the bulk concentrations of the oxidized and reduced species, respectively. α_c and α_a are the apparent transfer coefficients for the cathodic (reduction) and anodic (oxidation) reactions. They represent the fractional amount that each reaction is favored under an applied overpotential, η, and usually sum to unity for elementary, one-electron reactions.

One of the simplest methods for estimating i_0 is electrochemical impedance spectroscopy (EIS), which probes the interfacial resistance between a reversible electrode, such as lithium metal, and an electrolyte. If the measured resistance is dominated by charge-transfer resistance, R_{ct}, then i_0 can be calculated simply as:

$$i_0 = \frac{RT}{FR_{ct}}. \quad (12)$$

EIS was conducted on Li–PEO/LiTFSI–Li cells as a function of temperature. i_0 of the Li/Li$^+$ reaction was determined with Arrhenius parameters based on Equation 12 and is reported in **Table III**.[55] This approach has also been applied to a composite electrolyte composed of a PEO electrolyte matrix and γ-$LiAlO_2$ ceramic particles.[56] R_{ct} was determined based on a deconvolution of EIS data and i_0 (reported in Table III) was found to be significantly lower than reports for PEO. This highlights an important limitation of the EIS approach. The assumption that charge-transfer resistance dominates is tenuous considering the possibility of contact resistance and formation of solid electrolyte interphases due to spontaneous reaction between electrolyte and lithium.

Another approach to measure i_0 is potential step voltammetry in which a current measurement is taken at a constant applied voltage. Equivalently, galvanostatic polarization (current-controlled measurement) was used in older literature due to the difficulty of controlling voltage with instruments in use at the time. When a potential is applied to a cell originally at rest, the ensuing current can be decomposed into a capacitive current, due to the rate of potential change, and a Faradaic current, due to charge transfer between electrode and electrolyte. The capacitive current acts to charge the electric double layer that exists at the electrode–electrolyte interface, but does not drive a reaction. The Faradaic current, on the other hand, is due to electrochemical reactions and is relevant for an operating battery. The primary disadvantage of galvanostatic polarization is that the voltage changes throughout the experiment, so that measurements are not purely Faradaic. With potential step voltammetry, capacitive charging decays rapidly.

With solid electrolytes, a rest step between measurements allows the cell to return to an equilibrium state via diffusion, which dissipates any concentration gradients that were generated by the previous measurement.[57] The length of the rest step is related to Ne. For sufficiently slow reactions (with respect to diffusion) and sufficiently small applied overpotentials, reaction kinetic control can be maintained. The results of a representative study using galvanostatic polarization to measure i_0 of Li/Li$^+$ reaction kinetics in PEO electrolyte is reported in the second row of Table III.[58] This approach can also be applied to kinetics of other electrodes[59] and electrolyte degradation reactions.[57]

If all transport parameters of an electrolyte are known, then battery cycling can be phenomenologically modeled using i_0

Table III. Exchange current density from various methods for lithium plating/stripping with specified electrolyte.

System	T (°C)	m (mol/kg)	i_0 (mA/cm^2)	Method
PEO + LiTFSI	90	1.5	4.1	EIS
PEO + $LiCF_3SO_3$	100	2.5	0.96	Galvanostatic Polarization
		2.0	1.54	
SEO + LiTFSI	90	1.9	0.55	Modeling
PEO + $LiBF_4$ + γ-$LiAlO_2$	90	1.1	0.1	EIS

Note: PEO, poly(ethylene oxide); LiTFSI, lithium bis(trifluoromethanesulfone)-imide; SEO, polystyrene-*block*-polyethylene oxide electrolyte.

as an adjustable parameter. In fact, i_0 for lithium plating and stripping has been determined by regressing a full cell model to constant-current cycling data from Li–SEO/LiTFSI–Li cells.[60] Despite constant transport parameters being used in the model, i_0 from this study compares reasonably well with the other reports in Table III.

Considering the differences in PEO molecular weight, anion type, and lithium metal surface preparation methods (causing uncertainty in the contact and passivation layer resistances at the Li–electrolyte interface), the agreement in Table III is remarkable. i_0 between Li and PEO-based electrolytes is on the order of 1 mA/cm^2. Interestingly, this is similar in magnitude to that reported for a carbonate-based liquid electrolyte used in lithium-ion batteries,[61] but an order of magnitude lower than an ether-based liquid electrolyte[62] and an inorganic solid electrolyte.[63]

Conclusions

Composite polymer electrolytes allow material combinations that can address processing challenges, maintain adhesion during battery cycling, and enable higher charge and discharge rates. There is much, however, to be done in order to build a framework that predicts battery performance in composite electrolytes, not to mention the rapid recent development of new electrolyte materials. We have attempted to provide a simple starting point upon which such a framework might be built. A key component of the framework is the Newman number that, in conjunction with conductivity, provides a prediction of electrolyte performance at low rates. Ultimately, predicting the performance of electrolytes at high charge and discharge rates requires knowledge of the dependence of transport and thermodynamic properties (κ, D, t_+^0, and T_h) as a function of salt concentration.

The effective medium approach enables calculation of transport and thermodynamic properties of composite electrolytes with one conducting phase in terms of the volume fraction of the conducting phase. It must be recognized that the effective medium model is only a starting point that does not address factors such as interparticle interactions and resistance between grains. It is not straightforward to extend effective medium framework to composites with two ion-conducting phases. Even for the simple case of single-ion conductors dispersed in a conventional binary polymer electrolyte, the six transport coefficients necessary to characterize the system have not yet been identified. We expect the transport number mismatch between the phases to have a large effect on ion transport. We conclude by noting the importance of quantifying reaction kinetics in addition to measuring transport parameters of electrolytes for predicting the charge-discharge behavior of lithium batteries containing solid electrolytes. This is particularly challenging in solid electrolytes due to the lack of convection.

Lithium-ion technology based on transition-metal oxide cathodes, graphite anodes, and carbonate-based liquid electrolytes provides hope for powering the emerging clean-energy landscape. In spite of the challenges that remain, solid electrolytes offer the most promising approach to improve upon this technology, as stated by Goodenough and co-workers in 1980.

Acknowledgments

This work was supported by the Joint Center for Energy Storage Research, an Energy Innovation Hub funded by the US Department of Energy, Office of Science, Basic Energy Sciences, under Contract No. DEAC02–06CH11357. D.H. acknowledges support from NSF CAREER Award No. 1751450 and NSF CREST Award No. 1735968, as well as the LG Chem Battery Innovation Contest.

References

1. K. Mizushima, P.C. Jones. P.J. Weisman, J.B. Goodenough, *Mater. Res. Bull.* **15**, 783 (1980).
2. W.S. Harris, "Electrochemical Studies in Cyclic Esters," PhD thesis, University of California, Berkeley (1958).
3. R. Fong, U. Von Sacken, J.R. Dahn, *J. Electrochem. Soc.* **137**, 2009 (1990).
4. D.E. Fenton, J.M. Parker, P.V. Wright, *Polymer* **14**, 589 (1973).
5. M.B. Armand, *Annu. Rev. Mater. Sci.* **16**, 245 (1986).
6. P.G. de Gennes, *Scaling Concepts in Polymer Physics* (Cornell University Press, Ithaca, NY, 1979).
7. P.J. Flory, *Principles of Polymer Chemistry* (Cornell University Press, Ithaca, NY, 1953).
8. R. Mercier, J.P. Malugani, B. Fahys, G. Robert, *Solid State Ionics* **5**, 663 (1981).
9. H. Wada, M. Menetrier, A. Levasseur, P. Hagenmuller, *Mater. Res. Bull.* **18**, 189 (1983).
10. N. Kamaya, K. Homma, Y. Yamakawa, M. Hirayama, R. Kanno, M. Yonemura, T. Kamiyama, Y. Kato, S. Hama, K. Kawamoto, A. Mitsui, *Nat. Mater.* **10**, 682 (2011).
11. Z. Liu, W. Fu, E.A. Payzant, X. Yu, Z. Wu, N.J. Dudney, J. Kiggans, K. Hong, A.J. Rondinone, C. Liang, *J. Am. Chem. Soc.* **135**, 975 (2013).
12. Z. Zhang, J.H. Kennedy, *Solid State Ionics* **38**, 217 (1990).
13. C. Monroe, J. Newman, *J. Electrochem. Soc.* **152**, A396 (2005).
14. J.S. Newman, K.E. Thomas-Alyea, *Electrochemical Systems*, 3rd ed. (Prentice-Hall, Englewood Cliffs, NJ, 2004).
15. Y.P. Ma, M. Doyle, T.F. Fuller, M.M. Doeff, L.C. De Jonghe, J. Newman, *J. Electrochem. Soc.* **142**, 1859 (1995).
16. D.M. Pesko, K. Timachova, R. Bhattacharya, M.C. Smith, I. Villaluenga, J. Newman, N.P. Balsara, *J. Electrochem. Soc.* **164**, E3569 (2017).
17. J. Shi, C.A. Vincent, *Solid State Ionics* **60**, 11 (1993).
18. A.A. Teran, M.H. Tang, S.A. Mullin, N.P. Balsara, *Solid State Ionics* **203**, 18 (2011).
19. P.G. Bruce, C.A. Vincent, *J. Electroanal. Chem.* **225**, 1 (1987).
20. M. Watanabe, M. Rikukawa, K. Sanui, N. Ogata, *J. Appl. Phys.* **58**, 736 (1985).
21. M. Doyle, J. Newman, *J. Electrochem. Soc.* **142**, 3465 (1995).
22. N.P. Balsara, J. Newman, *J. Electrochem. Soc.* **162**, A2720 (2015).
23. I. Villaluenga, K.H. Wujcik, W. Tong, D. Devaux, D.H.C. Wong, J.M. DeSimone, N.P. Balsara, *Proc. Natl. Acad. Sci. U.S.A.* **113**, 52 (2016).
24. X.G. Sun, C.L. Reeder, J.B. Kerr, *Macromolecules* **37**, 2219 (2004).
25. R. Bouchet, S. Maria, R. Meziane, A. Aboulaich, L. Lienafa, J.P. Bonnet, T.N.T. Phan, D. Bertin, D. Gigmes, D. Devaux, R. Denoyel, M. Armand, *Nat. Mater.* **12**, 452 (2013).
26. M. Doyle, T.F. Fuller, J. Newman, *Electrochim. Acta* **39**, 2073 (1994).
27. D.T. Hallinan, N.P. Balsara, *Annu. Rev. Mater. Res.* **43**, 503 (2013).
28. D.M. Pesko, Y. Jung, A.L. Hasan, M.A. Webb, G.W. Coates, T.F. Miller, N.P. Balsara, *Solid State Ionics* **289** 118 (2016).
29. S. Lascaud, M. Perrier, A. Vallee, S. Besner, J. Prudhomme, M. Armand, *Macromolecules* **27**, 7469 (1994).
30. O. Oparaji, S. Narayanan, A. Sandy, S. Ramakrishnan, D. Hallinan, *Macromolecules* **51**, 2591 (2018).
31. J. Sax, J.M. Ottino, *Polym. Eng. Sci.* **23**, 165 (1983).
32. I. Villaluenga, X.C. Chen, D. Devaux, D.T. Hallinan, N.P. Balsara, *Macromolecules* **48**, 358 (2015).
33. K.-H. Shen, J.R. Brown, L.M. Hall, *ACS Macro Lett.* **7**, 1092 (2018).
34. G. Desmet, S. Deridder, *J. Chromatogr. A* **1218**, 32 (2011).
35. J.C. Maxwell, *Treatise on Electricity and Magnetism*, 3rd ed. (Academic Reprints, Stanford, CA, 1953), vol. 1.

36. S. Torquato, *Random Heterogeneous Materials: Microstructure and Macroscopic Properties* (Springer, New York, 2013).
37. M.W. Matsen, F.S. Bates, *Macromolecules* **29**, 1091 (1996).
38. E.W. Cochran, C.J. Garcia-Cervera, G.H. Fredrickson, *Macromolecules* **39**, 2449 (2006).
39. I. Villaluenga, D.M. Pesko, K. Timachova, Z. Feng, J. Newman, V. Srinivasan, N.P. Balsara, *J. Electrochem. Soc.* **165**, A2766 (2018).
40. F. Croce, G.B. Appetecchi, L. Persi, B. Scrosati, *Nature* **394**, 456 (1998).
41. D. Golodnitsky, G. Ardel, E. Peled, *Solid State Ionics* **147**, 141 (2002).
42. I. Gurevitch, R. Buonsanti, A.A. Teran, B. Gludovatz, R.O. Ritchie, J. Cabana, N.P. Balsara, *J. Electrochem. Soc.* **160**, A1611 (2013).
43. A.P. Gast, L. Leibler, *Macromolecules* **19**, 686 (1986).
44. D.A.G. Bruggeman, *Ann. Phys.* **416**, 636 (1935).
45. I.V. Thorat, D.E. Stephenson, N.A. Zacharias, K. Zaghib, J.N. Harb, D.R. Wheeler, *J. Power Sources* **188**, 592 (2009).
46. Y. Seino, T. Ota, K. Takada, A. Hayashi, M. Tatsumisago, *Energy Environ. Sci.* **7**, 627 (2014).
47. Y. Kato, S. Hori, T. Saito, K. Suzuki, M. Hirayama, A. Mitsui, M. Yonemura, H. Iba, R. Kanno, *Nat. Energy* **1**, 16030 (2016).
48. M. Keller, G.B. Appetecchi, G.-T. Kim, V. Sharova, M. Schneider, J. Schuhmacher, A. Roters, S. Passerini, *J. Power Sources* **353**, 287 (2017).
49. S. Skaarup, K. West, P.M. Julian, D.M. Thomas, *Solid State Ionics* **40–1**, 1021 (1990).
50. D.R. MacFarlane, P.J. Newman, K.M. Nairn, M. Forsyth, *Electrochim. Acta* **43**, 1333 (1998).
51. J. Zheng, Y.-Y. Hu, *ACS Appl. Mater. Interfaces* **10**, 4113 (2018).
52. A. Mehrotra, P.N. Ross, V. Srinivasan, *J. Electrochem. Soc.* **161**, A1681 (2014).
53. M. Schleutker, J. Bahner, C.L. Tsai, D. Stolten, C. Korte, *Phys. Chem. Chem. Phys.* **19**, 26596 (2017).
54. A.J. Bard, L.R. Faulkner, *Electrochemical Methods, Fundamentals and Applications* (Wiley, New York, 2001).
55. P.F. Driscoll, L. Yang, M. Gervais, J.B. Kerr, *ECS Trans.* **33**, 33 (2011).
56. B. Scrosati, F. Croce, S. Panero, *J. Power Sources* **100**, 93 (2001).
57. D.T. Hallinan Jr., A. Rausch, B. McGill, *Chem. Eng. Sci.* **154**, 34 (2016).
58. C.A.C. Sequeira, A. Hooper, *Solid State Ionics* **9–10**, 1131 (1983).
59. A. Swiderska-Mocek, A. Lewandowski, *J. Solid State Electrochem.* **21**, 1365 (2017).
60. S.-L. Wu, A.E. Javier, D. Devaux, N.P. Balsara, V. Srinivasan, *J. Electrochem. Soc.* **161**, A1836 (2014).
61. R. Jasinski, in *Advances in Electrochemistry and Electrochemical Engineering*, P. Delahey, C.W. Tobias, Eds. (Interscience, New York, 1971), vol. 8, pp. 253–335.
62. W.M. Hedges, D. Pletcher, *J. Chem. Soc. Faraday Trans. 1* **82**, 179 (1986).
63 M. Chiku, W. Tsujiwaki, E. Higuchi, H. Inoue, *J. Power Sources* **244**, 675 (2013). □

Daniel T. Hallinan Jr. is an assistant professor of chemical engineering at the Florida A&M University–Florida State University College of Engineering. He received his bachelor's degrees from Lafayette College and his PhD degree from Drexel University. He was a postdoctoral fellow at Lawrence Berkeley National Laboratory and the University of California, Berkeley. His current research focuses on fundamental polymer physics of nanostructured materials, as well as applications related to energy sustainability. Hallinan is actively involved in the polymer communities of the American Physical Society and the American Institute of Chemical Engineers. He recently received an NSF CAREER Award and has testified before a US congressional subcommittee in support of national synchrotron facilities. Hallinan can be reached by email at dhallinan@fsu.edu.

Irune Villaluenga is an electrolyte chemist at Blue Current, a battery startup company, located in Berkeley, California. She obtained her bachelor's degree in 2005 and her PhD degree in chemistry in 2010, both from the University of the Basque Country, Spain. She was a postdoctoral researcher at CIC Energigune, Spain, and Lawrence Berkeley National Laboratory. In 2017, she worked as a project scientist at Lawrence Berkeley National Laboratory. Her current research interests include inorganic, polymer, and composite electrolytes for battery applications. Villaluenga can be reached by email at irvillaluenga@gmail.com.

Nitash P. Balsara is a chemical engineer at the University of California, Berkeley. He received his bachelor's degree from the Indian Institute of Technology in Kanpur, India, his master's degree from Clarkson University, and his PhD degree from Rensselaer Polytechnic Institute. This was followed by two postdoctoral appointments at the University of Minnesota and the Exxon Research and Engineering Company. In 1992, he joined the faculty of the Department of Chemical Engineering at Polytechnic University in New York. In 2000, he moved to Berkeley to join the faculty of the Department of Chemical Engineering at the University of California and to join Lawrence Berkeley National Laboratory as a faculty scientist. He co-founded two battery startups, Seeo and Blue Current. Balsara can be reached by email at nbalsara@berkeley.edu.